Bioprocess and Biosystems Engineering (2022) 45:365–380
https://doi.org/10.1007/s00449-021-02666-9

RESEARCH PAPER

Green synthesis of silver nanoparticles using *Rhodiola imbricata* and *Withania somnifera* root extract and their potential catalytic, antioxidant, cytotoxic and growth-promoting activities

Sahil Kapoor[1,2,3] · Hemant Sood[2] · Shweta Saxena[1] · Om Prakash Chaurasia[1]

Received: 21 August 2021 / Accepted: 10 November 2021 / Published online: 6 January 2022

Abstract

This study presents the development of a sustainable production process of environmentally benign silver nanoparticles (AgNPs) from aqueous root extract of *Rhodiola imbricata* (RI) and *Withania somnifera* (WS) for mitigating environmental pollution and investigating their potential applications in agriculture and biomedical industry. RIWS-AgNPs were characterized using several analytical techniques (UV–Vis, DLS, HR-TEM, SAED, EDX and FTIR). The antioxidant and anticancer activity of RIWS-AgNPs were estimated by DPPH and MTT assay, respectively. UV–Vis and DLS analysis indicated that equal ratio of RIWS-extract and silver nitrate (1:1) is optimum for green synthesis of well-dispersed AgNPs (λ_{max}: 430 nm, polydispersity index: 0.179, zeta potential: − 17.9 ± 4.14). HR-TEM and SAED analysis confirmed the formation of spherical and crystalline RIWS-AgNPs (37–42 nm). FTIR analysis demonstrated that the phenolic compounds are probably involved in stabilization of RIWS-AgNPs. RIWS-AgNPs showed effective catalytic degradation of hazardous environmental pollutant (4-nitrophenol). RIWS-AgNPs treatment significantly increased the growth and photosynthetic pigments of *Hordeum vulgare* in a size- and dose-dependent manner (germination (77%), chlorophyll a (12.62 ± 0.07 µg/ml) and total carotenoids (7.05 ± 0.04 µg/ml)). The DPPH assay demonstrated that RIWS-AgNPs exert concentration-dependent potent antioxidant activity (IC_{50}: 12.30 µg/ml, EC_{50}: 0.104 mg/ml, ARP: 959.45). Moreover, RIWS-AgNPs also confer strong cytotoxic activity against HepG2 cancer cell line in dose-dependent manner (cell viability: 9.51 ± 1.55%). Overall, the present study for the first time demonstrated a green technology for the synthesis of stable RIWS-AgNPs and their potential applications in biomedical and agriculture industry as phytostimulatory, antioxidant and anticancer agent. Moreover, RIWS-AgNPs could potentially be used as a green alternative for environmental remediation.

✉ Hemant Sood
hemant.sood@juit.ac.in; hemant.sood2013@gmail.com

Sahil Kapoor
sahil.kapoor@ggdsd.ac.in; skpuindia7@gmail.com

[1] Defence Institute of High-Altitude Research (DRDO), C/O 56 APO, Leh-Ladakh, Jammu & Kashmir 901205, India

[2] Department of Biotechnology and Bioinformatics, Jaypee University of Information Technology, Waknaghat, Solan, Himachal Pradesh 173215, India

[3] Present Address: Department of Botany, Goswami Ganesh Dutta Sanatan Dharma College, Chandigarh 160030, India

Graphical abstract

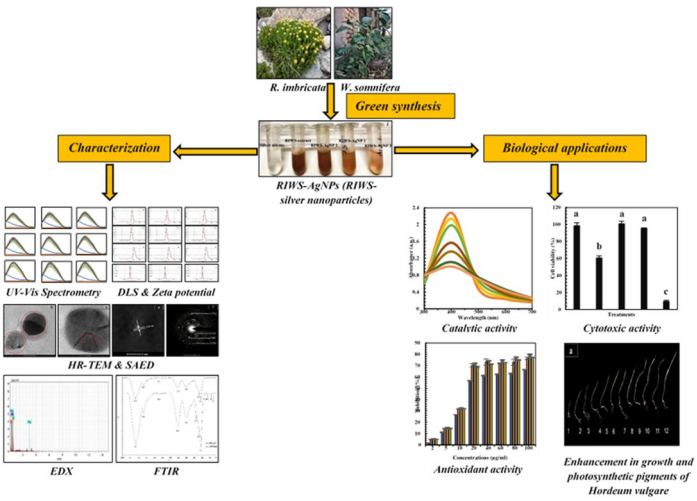

Keywords *Rhodiola imbricata* · *Withania somnifera* · Silver nanoparticles · Green synthesis · Antioxidant activity

Introduction

Among the various metallic nanoparticles (MNPs), silver nanoparticles (AgNPs) have garnered prodigious interest during recent years due to their unique physicochemical and biological properties [1]. It is estimated that nearly 500 tons of AgNPs are produced every year and the global market of AgNPs is expected to reach $ 2.45 billion by 2022 [2, 3]. AgNPs (1–100 nm) have broad applicability in the field of physics, chemistry, biology, medicine and material science [4–6]. AgNPs have high electrical and thermal conductivity, good chemical stability and pronounced optical, catalytic, magnetic and biological properties owing to their high surface-to-volume ratio [7–9]. Due to these distinct properties, the AgNPs are widely used in several different products, including textile coatings [1], food storage containers, air filters, deodorants, toothpaste [10, 11], bone cement, surgical instruments, surgical masks [12], wound dressings, tissue scaffolds, intermittent catheters, orthopedic prostheses [13], topical creams, antiseptic sprays and other medical and pharmaceutical products [1, 14].

AgNPs are generally synthesized by top-down or bottom-up approach [15]. These approaches encompass physical, chemical and biological methods for the preparation of these AgNPs. However, the physical and chemical methods are inefficacious, exorbitant, unsustainable, high-energy demanding, labor-intensive, time-consuming and detrimental to the environment [9, 16–18]. Therefore, this necessitates the development of a cost-effective and eco-friendly approach for production of these AgNPs. Green nanobiotechnology using biological systems (plants and microorganisms) offer a suitable alternative source for the synthesis of AgNPs. This green technology of fabricating AgNPs is immensely beneficial over chemical and physical methods as it is fast, energy efficient, economical, environmentally benign, robust, reliable and relatively reproducible process [16, 19, 20]. The major mechanism behind the plant extract-mediated biosynthesis of AgNPs is phytochemicals-assisted reduction of silver ions into silver nanoparticles [21]. Recently, AgNPs have been successfully fabricated using the extract of different plant species, including *Ammania baccifera* [22], *Citrullus lanatus* [23] and *Momordica charantia* [24].

Withania somnifera (L.) Dunal. (Ashwagandha, Family: Solanaceae) is an important medicinal plant in the traditional Indian system of medicine for more than 3000 years [25]. *W. somnifera* (WS) is widely distributed in Asia, Africa, Middle East and Mediterranean region [26]. In India, it grows mostly in Punjab, Jammu and Himachal Pradesh [27]. About 2000 tons of Ashwagandha roots are annually produced in India and the dried roots are sold at approximately $ 140 per quintal [28]. The root extract of *W. somnifera* is extensively used for the treatment of rheumatism, gynec disorders, bronchitis, arthritis, senile debility, tuberculosis and cardiac, skin and inflammatory diseases [29–31]. It also possesses a wide array of therapeutic properties, including anti-inflammatory, anti-tumor, anti-bacterial, antispasmodic, hypoglycemic and hypolipidemic effects [32, 33]. These therapeutic properties have been mainly attributed to its diverse array of secondary metabolites, including steroidal lactones (withaferin A, withanolide A, withanolide D, withanolide B), flavonoids

and phenolics (dihydroxykaempferol, quercetin, quercetin-3-rutinoside, quinic acid, scopoletin and aesculentin), tropane alkaloids (tropine, pseudotropine, nicotine, withasomine, anaferine), withanone, ashwangandholide, withanolide dimer sulphide, 2,3 dihydrowithaferin A (viscosalactone B) and 27-hydroxywithanolide A [34–36].

Rhodiola imbricata Edgew. (Shrolo, Family: Crassulaceae) is a highly valuable medicinal plant in the traditional Tibetan and Amchi system of medicine [37]. It grows at high-altitude passes (Changla, Khardungla and Penzila) of trans-Himalayan Ladakh region [38]. *R. imbricata* (RI) is widely used for the treatment of fever, cough, cold, cardiac and nervous system disorders [37]. The roots of *R. imbricata* contain several bioactive compounds, including phenolic compounds (salidroside, tyrosol, gallic acid, rosavins, cinnamyl alcohol, o-methylorcinol, p-hydroxybenzaldehyde, 4-methoxyphenethyl alcohol, 3-methyl-5-methoxyphenyl-β-D-glucopyranoside, 2-hydroxymethyl-6-methoxyphenyl-β-D-glucopyranoside, 3,5-dimethoxyphenyl-β-D-glucopyranoside), steroidal glycosides and terpenoids that have pronounced hepatoprotective, adaptogenic, antioxidant, cytoprotective, anticancer, antiviral, and immunostimulatory properties [37, 39–44]. *R. imbricata* root also contains different health-promoting attributes, including essential amino acids (histidine and lysine), fatty acids (capric acid, linoleic acid and oleic acid), dietary mineral elements (calcium and potassium), fat-soluble vitamins (alpha-tocopherol) and water-soluble vitamins (nicotinic acid, pantothenic acid and pyridoxine) [45, 46].

The biocompatibility, bioactivities and other properties and applications of plant derived AgNPs primarily depends on its shape, size and surface chemistry, which in turn are regulated by phyto-constituents (phenolics, flavonoids, terpenoids) present in the plant extract. However, the nature and concentrations of these phyto-constituents vary among different plant species. Therefore, keeping in view the phyto-constituents and pharmacological properties of *R. imbricata* and *W. somnifera*, the present study was focused on the cleaner production and characterization of AgNPs (ultraviolet–visible spectroscopy (UV–Vis), dynamic light scattering (DLS), high-resolution transmission electron microscopy (HR-TEM), selected area electron diffraction (SAED), energy-dispersive X-ray spectroscopy (EDX) and Fourier-transform infrared spectroscopy (FTIR)) from aqueous root extract of *R. imbricata* and *W. somnifera* for managing industrial pollution (catalytic degradation of 4-nitrophenol (4-NP)) and investigating their potential in biomedical (cytotoxicity against human hepatocellular carcinoma cell line (HepG2)), agricultural and bio-based (antioxidant) industrial sector. Moreover, the present study also investigated the influence of different ratio of RIWS aqueous root extract and silver nitrate ($AgNO_3$) on physicochemical properties and biological applications of RIWS-AgNPs.

Materials and methods

Chemicals

All the chemicals used in this study were of analytical grade. Double-distilled and Milli-Q (MQ) water was used throughout the study.

Green synthesis of RIWS-AgNPs

RIWS-AgNPs were synthesized according to previously established method with some minor modifications [23]. *R. imbricata* and *W. somnifera* plants were collected from Changla pass (Ladakh, India) and Togan village (Chandigarh, India), respectively. The roots of both the plants were washed thoroughly with double-distilled water (DDW) and then air-dried at room temperature (RT) for 15 days. Subsequently, the air-dried roots were pulverized and sieved through a 20-mesh sieve to obtain a fine powder. 5 g of *R. imbricata* root powder and 5 g of *W. somnifera* root powder was mixed thoroughly and dissolved in 100 ml of sterile MQ water and boiled at 60 °C for 25 min. After boiling, the extract was cooled down to RT and filtered twice through Whatman No. 1 filter paper. The extract was then re-filtered through 0.45 µm filter (Millex; Merck, Frankfurt, Germany) and stored at 4 °C. Subsequently, $AgNO_3$ (1 mM, 2.5 mM and 5 mM) and aqueous RIWS-extract (1 mg/ml) were mixed in different ratio (v/v) (Table 1) and reaction was allowed to progress at 25 °C in dark condition. The reaction mixture was monitored visually at regular intervals to observe the changes in the color with time for its subsequent characterization.

Characterization of RIWS-AgNPs

RIWS-AgNPs were characterized according to previously established method [47]. The size and specific localized surface plasmon resonance (LSPR) of RIWS-AgNPs (Table 1) was observed in the wavelength range of 300–700 nm at 30 min intervals up to 3 h using BioTek Synergy H1 microplate reader (BioTek Instruments, Winooski, VT, USA) equipped with Gen5 software. The hydrodynamic size, polydispersity index (PDI), surface charge (zeta potential) and stability of RIWS-AgNPs (Table 1) was measured using Zetasizer Nano ZS instrument (Malvern Panalytical Ltd., Malvern, UK) equipped with Zetasizer software (version 7.12). The morphological features (size and shape), SAED and nature of RIWS-AgNPs were ascertained using Tecnai TF20 HR-TEM (FEI, Hillsboro, OR, USA). The TEM grid was prepared by loading 5 µl of RIWS-AgNPs suspension on carbon-coated copper grid and subsequent drying at RT.

Table 1 RIWS-AgNPs phytosynthesized using different combinations and concentrations of $AgNO_3$ and RIWS-extract

S.no	RIWS-AgNP ID	RIWS-AgNP composition (RIWS-extract: $AgNO_3$ ratio (v/v))
1	RIWS-AgNP 1	1 (RIWS-extract (1 mg/ml)): 1 ($AgNO_3$ (1 mM))
2	RIWS-AgNP 2	9 (RIWS-extract (1 mg/ml)): 1 ($AgNO_3$ (1 mM))
3	RIWS-AgNP 3	1 (RIWS-extract (1 mg/ml)): 9 ($AgNO_3$ (1 mM))
4	RIWS-AgNP 4	1 (RIWS-extract (1 mg/ml)): 1 ($AgNO_3$ (2.5 mM))
5	RIWS-AgNP 5	9 (RIWS-extract (1 mg/ml)): 1 ($AgNO_3$ (2.5 mM))
6	RIWS-AgNP 6	1 (RIWS-extract (1 mg/ml)): 9 ($AgNO_3$ (2.5 mM))
7	RIWS-AgNP 7	1 (RIWS-extract (1 mg/ml)): 1 ($AgNO_3$ (5 mM))
8	RIWS-AgNP 8	9 (RIWS-extract (1 mg/ml)): 1 ($AgNO_3$ (5 mM))
9	RIWS-AgNP 9	1 (RIWS-extract (1 mg/ml)): 9 ($AgNO_3$ (5 mM))

The elemental composition of RIWS-AgNPs were ascertained using an EDX instrument attached to Hitachi SU8010 field emission scanning electron microscope (Hitachi High-Technologies Corporation, Tokyo, Japan). The functional groups of RIWS-AgNPs were characterized by Spectrum 400 FTIR spectrometer (PerkinElmer, Waltham, MA, USA) using KBr pellet method (scan range: 4000–650 cm^{-1} and resolution: 0.4 cm^{-1}).

Catalytic activity of RIWS-AgNPs

The catalytic degradation of 4-NP by RIWS-AgNPs was assessed using previously reported method with some minor modifications [47]. Briefly, 200 µl of RIWS-AgNP 1 (200 µg/ml) was added to 200 µl of 4-NP (10^{-5} M) and 2.5 ml of sodium borohydride (0.150 M) and absorbance of reaction mixture and blank was measured in the wavelength range of 300–700 nm at 30 min intervals up to 180 min using BioTek Synergy H1 microplate reader (BioTek Instruments, Winooski, VT, USA) equipped with Gen5 software. The degradation efficiency of 4-NP by RIWS-AgNPs was estimated using the following formulae:

$$R = \frac{Ao - A}{Ao} \times 100,$$

where R is the degradation efficiency, Ao and A corresponds to absorbance of dye at time $t = 0$ and $t = 180$ min, respectively.

Seed germination assay and estimation of growth and photosynthetic pigments of *Hordeum vulgare*

Seeds ($n = 400$) of *Hordeum vulgare* were washed thoroughly with DDW, and then immersed in 70% ethanol for 1 min and washed five times with sterile MQ water. Then, the seeds were surface sterilized with 0.02% w/v mercuric chloride solution (containing few drops of Tween-20) for 1 min and subsequently washed six times with sterile MQ water. The surface sterilized seeds ($n = 9$) were then soaked in different concentrations of RIWS-AgNPs (RIWS-AgNP 1 (2, 20 and 200 µg/ml), RIWS-AgNP 4 (2, 20 and 200 µg/ml), RIWS-AgNP 7 (2, 20 and 200 µg/ml), RIWS-extract (200 µg/ml) and $AgNO_3$ and were kept in dark at RT for 10 h. Then, the treated seeds were transferred to soil-filled seedling trays. Finally, the seed germination index (SGI), root and shoot length, root number and photosynthetic pigments (Chlorophyll a, Chlorophyll b and total carotenoids) were measured after 10 days of incubation under 25 °C and 16 h (light)/8 h (dark) photoperiod.

SGI was calculated according to the following formula:

$$SGI(\%) = \frac{Number\ of\ germinated\ seeds}{Total\ number\ of\ inoculated\ seeds} \times 100.$$

Chlorophyll a, Chlorophyll b and total carotenoids were extracted from leaves (acetone with 20% v/v water) and measured according to the method of Lichtenthaler and Buschmann [48] using the following formula:

$$Chlorophyll\ a(\mu g/ml) = 12.25A_{663.2} - 2.79A_{646.8}$$

$$Chlorophyll\ b(\mu g/ml) = 21.50A_{646.8} - 5.10A_{663.2}$$

$$Total\ carotenoids(\mu g/ml) = \left(1000A_{470} - 1.82c_a - 85.02c_b\right)/198.$$

Antioxidant activity of RIWS-AgNPs

The antioxidant activity of RIWS-extract, RIWS-AgNP 1 (2–100 µg/ml) and standards (BHT and Rutin) was determined by DPPH (2,2-diphenyl-1-picrylhydrazyl) assay [49]. The antioxidant activity was expressed as % inhibition of DPPH which was calculated using the following formula:

$$Inhibition(\%) = [(Abs_{control} - Abs_{sample})/(Abs_{control})] \times 100.$$

The efficiency concentration (EC_{50}) and antiradical power (ARP) of antioxidant was calculated according to the method of Prakash [50], Kroyer [51] and Dajanta [52] using the following formula:

$$EC_{50}(mg/ml) = IC_{50}/(DPPH) in\, mg/ml$$

$$ARP = 1/\left(EC_{50} \times 100\right).$$

Cytotoxic activity of RIWS-AgNPs

The cytotoxic activity of RIWS-AgNPs was evaluated against HepG2 and normal Huh7 cell line, respectively, using MTT assay [53]. Briefly, the HepG2 and Huh7 cells were cultured in Dulbecco's modified eagle medium containing 10% fetal bovine serum, and maintained at 37 °C, 95% air, 5% CO_2 and 100% relative humidity. Then, the cultured cells (100 µl and 10,000 cells/well) were seeded in 96-well plate and incubated at 37 °C and 5% CO_2 for 24 h. After incubation, 20 µl of different concentrations of RIWS-AgNP 1 (2, 20 and 200 µg/ml) and RIWS-extract (200 µg/ml) was added to each well in triplicates and incubated at 37 °C and 5% CO_2 for 24 h. The untreated cells were used as a control. After 24 h of incubation, 20 µl of MTT (5 mg/ml in phosphate buffer saline) was added to each well and incubated at 37 °C for 4 h. After incubation, the formazan crystals formed as a result of reduction of MTT by mitochondrial dehydrogenase was solubilized in dimethyl sulfoxide (100 µl/well) and the absorbance was measured at 570 nm (test wavelength) and 620 nm (reference wavelength) using Multiskan GO microplate reader (Thermo Fisher Scientific, Waltham, MA, USA). The cell viability was assessed using the following formula:

$$Cell\ viability(\%) = \frac{(Abs_{570(sample)} - Abs_{620(sample)})}{(Abs_{570(control)} - Abs_{620(control)})} \times 100.$$

Statistical analysis

Completely randomized design methodology was used to carry out all the experiments [54]. The experiments were performed in triplicates and the results were presented as mean ± standard deviation. The difference between the group means was assessed through one-way ANOVA and the Bonferroni post hoc test was used to deduce the pairwise comparison among group means ($p \leq 0.05$). The SPSS software (SPSS version 21.0, USA) was used to perform the statistical analysis.

Results and discussion

Synthesis and characterization of RIWS-AgNPs

UV–Vis spectroscopy is a relatively simple, sensitive, rapid and selective technique for the characterization of phytosynthesized AgNPs [21]. The AgNPs generally show a characteristic LSPR peak (400–480 nm) due to collective oscillation of conduction band electrons [55]. The LSPR phenomenon depends on the shape and size of nanoparticles [18]. The present study was focused on the characterization of RIWS-AgNPs using UV–Vis spectrometry. After 30 min of incubation, color of the reaction mixture ($AgNO_3$ and RIWS-extract) changed from dark brown to light brown, thereby indicating the synthesis of RIWS-AgNPs (Fig. 1j). This change in color of reaction mixture is generally attributed to LSPR effect and reduction of Ag^+ ions to Ag^0 by plant extract [56]. The time-course analysis revealed that the intensity of LSPR peaks increased steadily (Fig. 1a–i). The UV–Vis spectrometric analysis demonstrated that intensity of maximum absorbance increased with increasing ratio of $AgNO_3$: RIWS-extract and increasing concentrations of $AgNO_3$ (Fig. 1a–i). Moreover, the LSPR peaks were broader in shape as well as red shifted from a smaller to a higher wavelength, thereby indicating the formation of a small amount of large size poly-disperse AgNPs (Fig. 1a–i). This red shift of LSPR peaks is due to aggregation among nanoparticles, which results in coupling of LSPR peaks that changes the local refractive index of AgNPs [55]. The RIWS-AgNP 1 (1:1 ratio of $AgNO_3$ (1 mM) and RIWS-extract (1 mg/ml) (v/v)) showed blue shifted high intensity LSPR peaks (430 nm), thereby revealing the formation of a large amount of small size AgNPs (Fig. 1a). According to Henglein, the LSPR peak shifts to the blue wavelength when electrons are donated to the nanoparticles [57]. Similar results have also been previously reported [18]. These results strongly suggest that the optimum ratio of $AgNO_3$ and plant extract is an important factor that regulates the physicochemical properties of AgNPs. The present findings suggest that the 1:1 ratio of $AgNO_3$: RIWS extract and 1 mM of $AgNO_3$ is optimum for the synthesis of small size and well-dispersed RIWS-AgNPs.

Hydrodynamic size, polydispersity and surface charge of RIWS-AgNPs

Dynamic light scattering (Photon Correlation Spectroscopy) and zeta potential are the most accepted techniques for determining the surface charge, hydrodynamic size, polydispersity and stability of phytosynthesized nanoparticles [58]. These techniques depend on the interaction of light with suspended nanoparticles [8, 59]. As shown in Fig. 2a–i and Table 2, the z-average (d-nm) or mean hydrodynamic size of RIWS-AgNPs range from 118.6 to 2969 nm. The polydispersity index (PDI) of RIWS-AgNPs range from 0.171 to 1 (Table 2). The PDI of RIWS-AgNP 1, RIWS-AgNP 2 and RIWS-AgNP 3, was found to be 0.179, 0.201 and 0.174, respectively, which is much below 0.3, thereby indicating that the synthesized nanoparticles are well dispersed

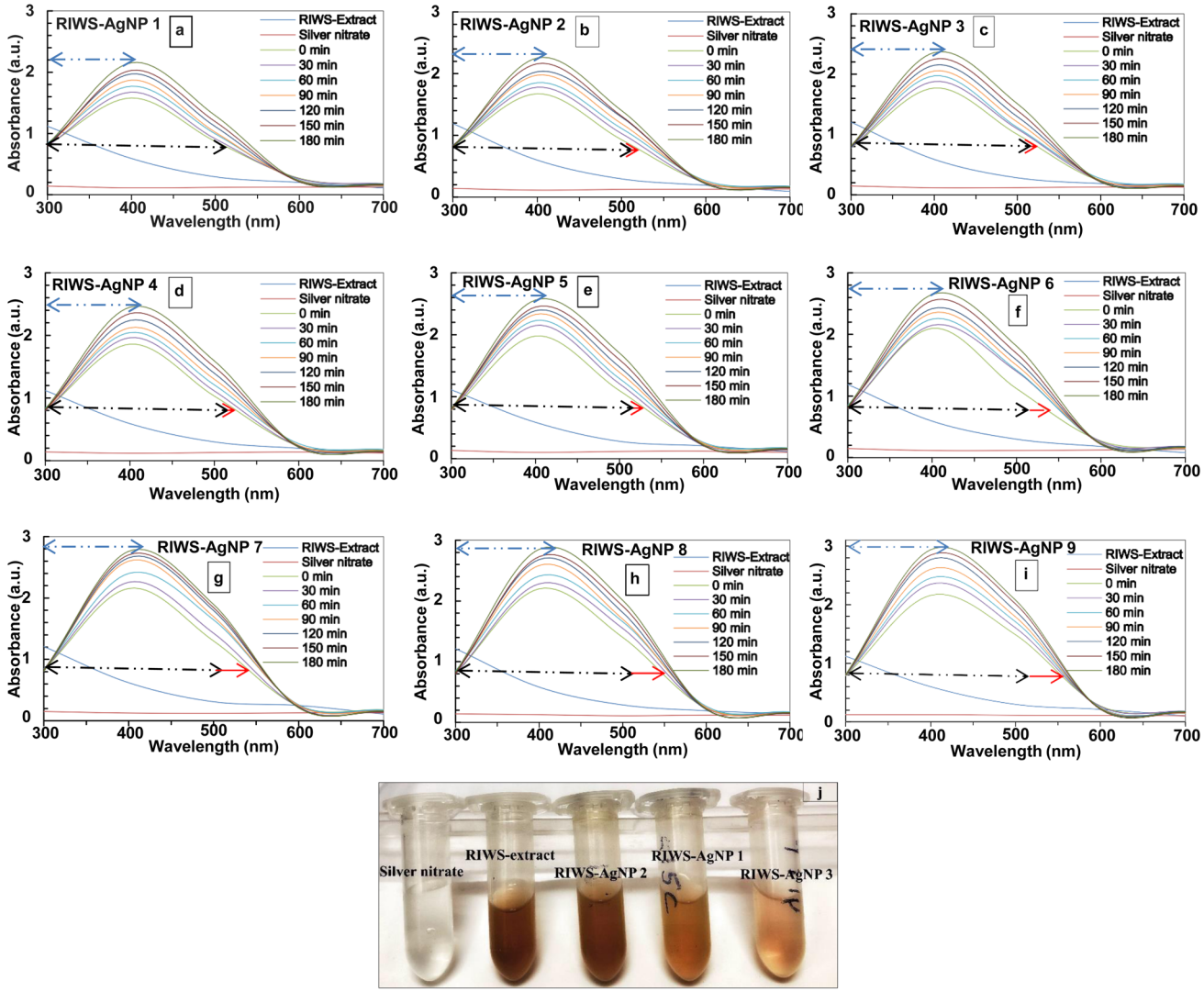

Fig. 1 UV–Vis absorption spectra of RIWS-AgNPs ((**a**) RIWS-AgNP 1, (**b**) RIWS-AgNP 2, (**c**) RIWS-AgNP 3, (**d**) RIWS-AgNP 4, (**e**) RIWS-AgNP 5, (**f**) RIWS-AgNP 6, (**g**) RIWS-AgNP 7, (**h**) RIWS-AgNP 8 and (**i**) RIWS-AgNP 9) and RIWS-extract over different time intervals. The black and red arrow indicates the increase in wavelength of RIWS-AgNPs ((**a**–**i**)). Blue arrow indicates the increase in absorbance of RIWS-AgNPs ((**a**–**i**)). (**j**) The figure shows the change in the color of reaction mixture ($AgNO_3$ and RIWS-extract)

in nature [60]. The results also suggest that the average hydrodynamic size and polydispersity of RIWS-AgNPs increased with increasing ratio of $AgNO_3$: RIWS-extract as well as increasing concentrations of $AgNO_3$. These findings also corroborate with the UV–Vis spectrometric results in this study. The zeta potential of RIWS-AgNP 1, RIWS-AgNP 2 and RIWS-AgNP 3 was found to be − 17.9 ± 4.14, − 14.5 ± 5.38 and − 5.20 ± 4.22 mV, respectively, indicating that the negative surface charge increased with increasing ratio of $AgNO_3$: RIWS-extract (Fig. 2j–l). The high negative surface charge on RIWS-AgNPs is due to prominent coating of RIWS root extract-derived phenolic hydroxyl (OH) groups on outer surface layer of these MNPs [22, 34–37, 39–42]. The high negative surface charge on RIWS-AgNP 1 exerts strong electrostatic repulsion among the nanoparticles that probably prevent agglomeration and impart long-term stability to these phytosynthesized AgNPs.

Spatial resolution of RIWS-AgNPs

HR-TEM is a powerful technique for understanding the spatial resolution of AgNPs. As shown in Fig. 3, the phytosynthesized RIWS-AgNPs are mostly spherical with an average size of 37–42 nm. Moreover, they are well dispersed, indicating that the phytosynthesized RIWS-AgNPs are stable against aggregation. These results also corroborate with the UV–Vis analysis in this study (Fig. 1). RIWS-AgNPs are probably capped by a thin layer of phyto-constituents

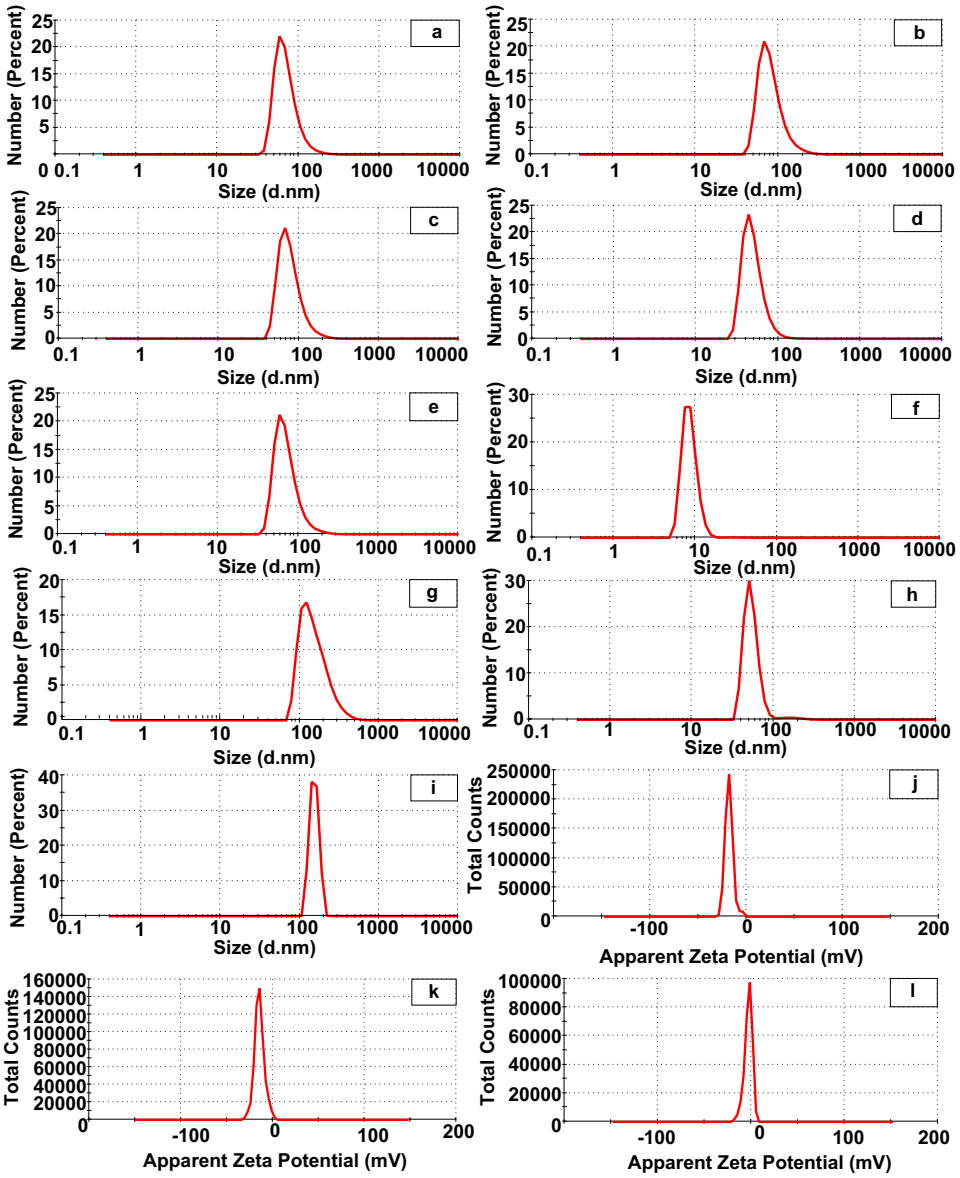

Fig. 2 Particle size distribution (DLS) ((**a**) RIWS-AgNP 1, (**b**) RIWS-AgNP 2, (**c**) RIWS-AgNP 3, (**d**) RIWS-AgNP 4, (**e**) RIWS-AgNP 5, (**f**) RIWS-AgNP 6, (**g**) RIWS-AgNP 7, (**h**) RIWS-AgNP 8 and (**i**) RIWS-AgNP 9) and Zeta potential ((**j**) RIWS-AgNP 1, (**k**) RIWS-AgNP 2, (**l**) RIWS-AgNP 3) of RIWS-AgNPs

Table 2 Z-Average and Polydispersity index of biosynthesized RIWS-AgNPs

S. No	RIWS-AgNP ID	*Z*-Average (d-nm)	Polydispersity index (PDI)
1	RIWS-AgNP 1	118.6	0.179
2	RIWS-AgNP 2	128.4	0.201
3	RIWS-AgNP 3	129.2	0.174
4	RIWS-AgNP 4	138.6	0.465
5	RIWS-AgNP 5	141.3	0.257
6	RIWS-AgNP 6	168.2	0.41
7	RIWS-AgNP 7	207.4	0.235
8	RIWS-AgNP 8	347.1	0.371
9	RIWS-AgNP 9	2969	1

from root extract of RIWS that render stability and prevents them from aggregation (Fig. 3a–d) [34–37, 39–42]. The interplanar "*d*" spacing of RIWS-AgNP was estimated to be 0.236 nm, which corresponds to the d111 lattice spacing of face-centered cubic structure (fcc) of silver (Fig. 3e). The SAED pattern illustrates circular fringes corresponding to (311), (220), (200) and (111) planes of fcc structure of silver which suggest that the phytosynthesized RIWS-AgNPs are crystalline in nature (Fig. 3f).

Elemental composition of RIWS-AgNPs

The elemental composition of AgNPs is generally established using EDX [58]. In this study, the EDX analysis shows a characteristic absorption peak of silver at 3 keV (Fig. 4) due to LSPR, thereby validating the formation

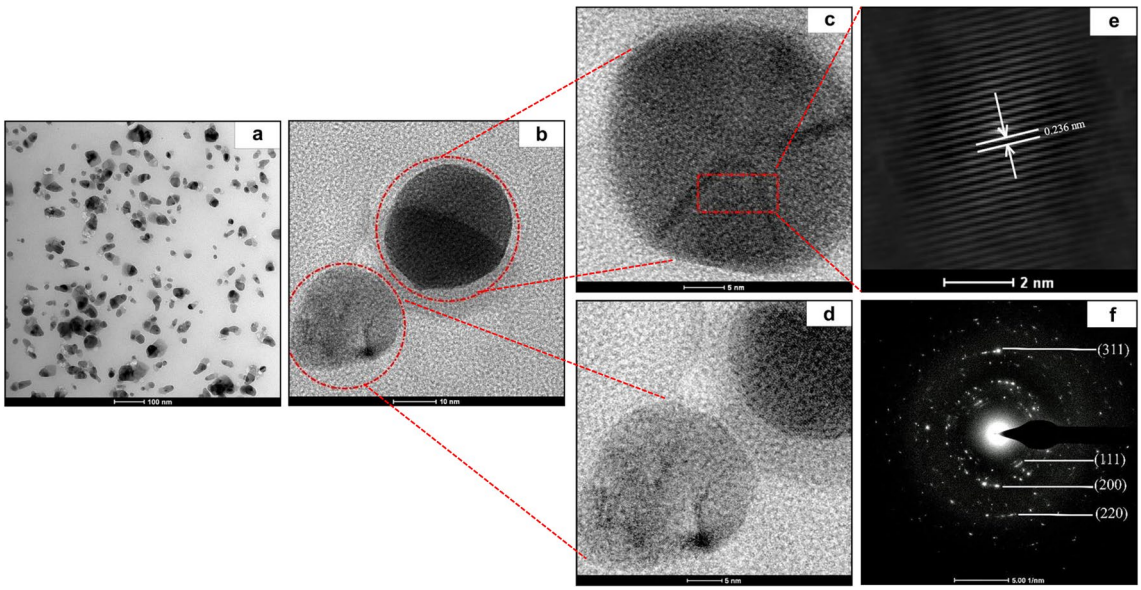

Fig. 3 HR-TEM images of RIWS-AgNP 1 at different resolutions ((**a**) 100 nm, (**b**) 10 nm, (**c**, **d**) 5 nm), and (**e**) interplanar "d" spacing; and (**f**) SAED pattern of RIWS-AgNPs

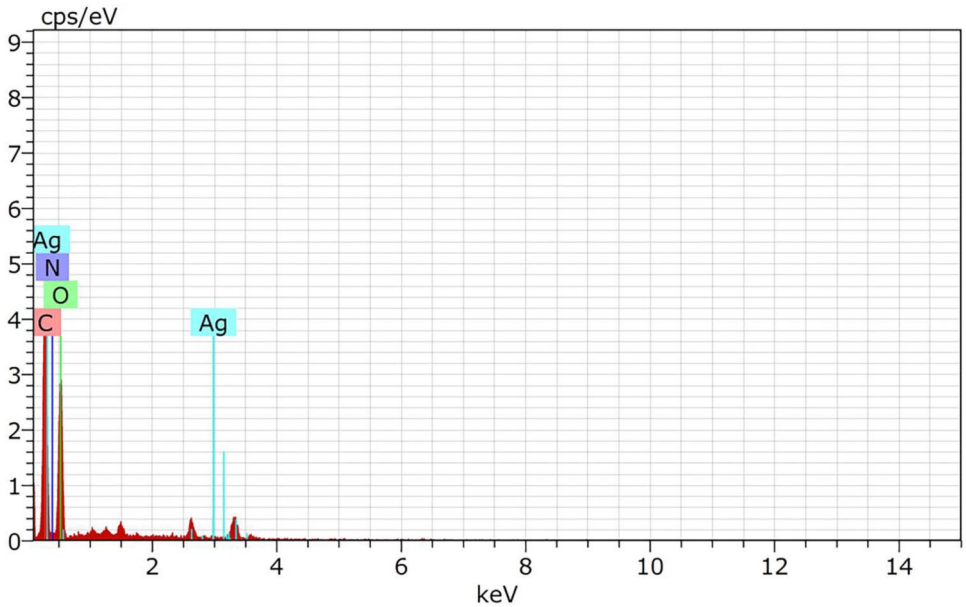

Fig. 4 EDX spectra showing the presence of silver, carbon, oxygen and nitrogen in RIWS-AgNPs

of RIWS-AgNPs [61]. Similar results have been previously reported in *Artocarpus heterophyllus* and *Ceratonia siliqua* leaf extract-derived AgNPs [62, 63]. The EDX analysis also demonstrated the presence of carbon, oxygen and nitrogen which could be ascribed to the phytoconstituents of RIWS root extract that are capped on the surface of AgNPs [34–37, 39–42].

Surface chemistry of RIWS-AgNPs

FTIR spectroscopy is widely used for characterizing the surface chemistry and functional groups involved in the reduction of silver ions [58]. In this study, the FTIR analysis of aqueous root extract of RIWS showed a spectrum of distinct IR band characteristic of O–H stretching of alcohols

and phenolic compounds (3329.1 cm^{-1}), C–H stretching of alkanes and aromatic compounds (2932.3 cm^{-1}), C≡C stretch of alkynes group (2153 cm^{-1}), C = C stretching of aromatic group (1601.3 cm^{-1}, 1399 cm^{-1}), C–O stretch of alcoholic, carboxylic acid, ester and ether functional sites of biomolecules (1148.7 cm^{-1}), C–N stretching of aliphatic amines or alcohols/phenols (1077.3 cm^{-1}, 1027.3 cm^{-1}), = C–H stretching of alkenes group (931.6 cm^{-1}), C–H bending of alkynes group (862.5 cm^{-1}), N–H stretch of 1° and 2° amines (766.9 cm^{-1}) and CH_2 (709.2 cm^{-1}) functional groups (Fig. 5) [64–66]. Whereas, the RIWS-AgNPs displayed IR band characteristic of O–H stretching of alcohols and phenolic compounds (3344.6 cm^{-1}), C–H stretching of alkanes and aromatic compounds (2930.7 cm^{-1}), C≡C stretch of alkynes group (2153.1 cm^{-1}), C = C stretching of aromatic group (1606 cm^{-1}, 1399.8 cm^{-1}), C–N stretching of aliphatic amines or alcohols/phenols (1076.8 cm^{-1}, 1030 cm^{-1}) functional groups (Fig. 5) [64–66]. The slight shift observed in IR band of RIWS-AgNPs spectra, as compared to the spectra of RIWS-extract, might be attributed to the phenolic functional groups present in the aqueous root extract of RIWS that probably act as reducing, capping and stabilizing agent for green synthesis of these AgNPs (Fig. 5) [30, 34–37, 39–42].

Catalytic activity of RIWS-AgNPs

4-NP is primarily used in production of pharmaceuticals, dyes, fungicides, insecticides and pesticides [67, 68]. It is listed as a toxic pollutant by the United States Environmental Protection Agency [69]. The short-term ingestion of 4-NP in humans causes cyanosis, drowsiness, nausea and headaches [68]. The 4-NP is resistant to biological and chemical hydrolysis due to presence of an electron withdrawing nitro group and is of great environmental concern [70]. Therefore, new technologies are still constantly developing to remove this hazardous pollutant from the environment. Recently,

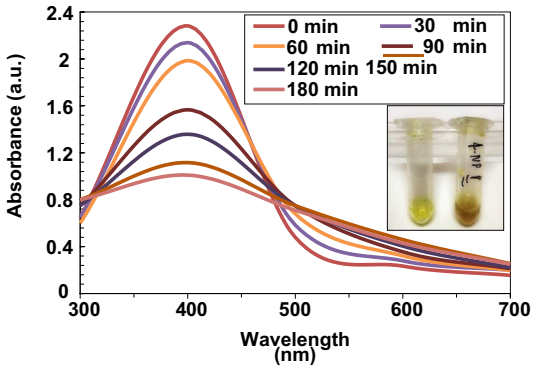

Fig. 6 UV–Vis absorption spectra showing catalytic degradation of 4-Nitrophenol by RIWS-AgNPs at different time intervals. The inset indicates the change in the color of reaction mixture after 30 min

there has been an increased attention towards the catalytic applications of AgNPs [71]. The catalytic activity of AgNPs usually depends on its shape, size and composition [72]. Therefore, the present study investigated the influence of RIWS-AgNPs on catalytic degradation of 4-NP. The addition of $NABH_4$ and RIWS-AgNPs resulted in reduction of 4-nitrophenolate ion to 4–aminophenol as indicated by the change in the color of reaction mixture (Fig. 6) [73]. The degradation efficiency of 4-NP by RIWS-AgNPs was found to be 57%. The UV–Vis analysis demonstrated an efficient catalytic degradation of 4-NP as evident by a considerable decrease in absorbance peak of 4-NP at the end of 30 min, 60 min, 120 min, 150 min and 180 min time interval (Fig. 6). This decrease in absorbance peak of 4-NP is mainly attributed to the large surface area of MNPs that act as substrate for electron transfer reaction or electron relay effect [74]. This decrease could also be explained on the basis of Langmuir–Hinshelwood model, which suggests that borohydride ions can transfer surface-hydrogen species to MNPs and subsequent adsorption of 4-NP on MNPs leads to catalytic

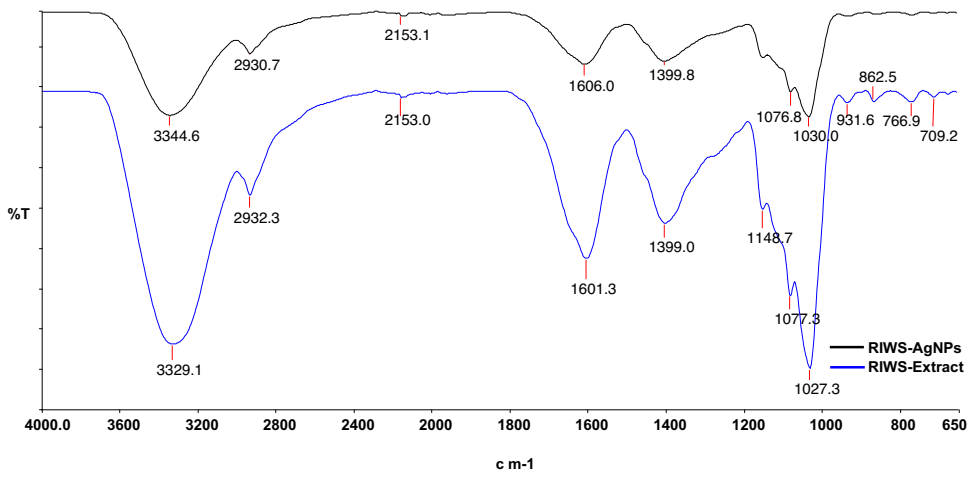

Fig. 5 FTIR spectra of RIWS-extract and RIWS-AgNPs

degradation of 4-NP by surface-hydrogen species [75]. Francis et al. [76] also reported similar catalytic degradation of 4-NP from *Elephantopus scaber*-derived AgNPs. The present findings suggest that RIWS-extract-derived AgNPs is a promising green alternative source of MNPs for treating toxic environmental pollutant.

Effect of RIWS-AgNPs on seed germination, growth and photosynthetic pigments of *Hordeum vulgare*

Recently, plant extract-derived AgNPs have gained tremendous popularity in agricultural sector [77]. Several studies have demonstrated the positive and negative effect of phytosynthesized AgNPs on plant growth and development [78]. The effect of AgNPs on plant growth generally depends on its size, concentration, source of nanoparticles and plant species under investigation [77]. Therefore, the present study investigated the influence of different concentrations of RIWS-AgNPs on germination, growth and photosynthetic pigments of *Hordeum vulgare*. As shown in Fig. 7a–d, the RIWS-AgNP 1 (200 µg/ml) treatment significantly increased the germination index (77%), root number (7.33 ± 0.25), shoot length (17.29 ± 0.41 cm) and content of photosynthetic pigments (chlorophyll a (12.62 ± 0.07 µg/ml), chlorophyll b (8.14 ± 0.02 µg/ml), total carotenoids (7.05 ± 0.04 µg/ml)) in *H. vulgare*, as compared to the other concentrations of RIWS-AgNPs and control ($p \leq 0.05$). However, the higher concentrations of RIWS-AgNPs have a negative impact on growth and photosynthetic pigments of *H. vulgare* (Fig. 7a–d). Therefore, the results suggest that the effect of RIWS-AgNPs on germination, growth and photosynthetic pigments of *H. vulgare* is mainly dependent on its concentration and physicochemical properties (size and zeta potential). Gupta et al. [77] also reported similar stimulatory effect of phytosynthesized AgNPs on seed germination, chlorophyll a, carotenoids content and seedling growth in rice. The authors found that AgNPs treatment significantly increased the levels of catalase, ascorbate peroxidase and glutathione reductase and substantially decreased the levels of hydrogen peroxide and lipid peroxidation, which in turn have enhanced the growth and germination in rice seedlings by increasing the efficiency of redox reactions. AgNPs treatment also significantly increased the root growth in rice and *Arabidopsis* due to its interaction with multiple cellular

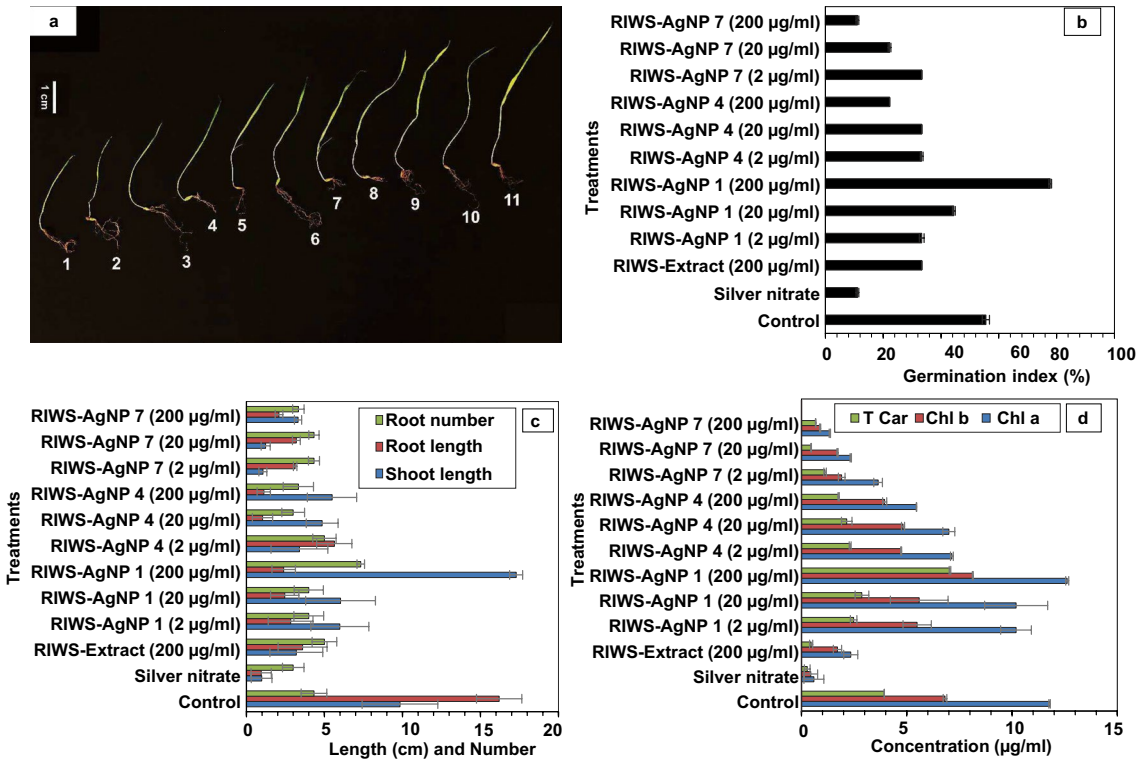

Fig. 7 Effect of RIWS-extract-derived AgNPs (RIWS-AgNP 1—RIWS-AgNP 9), RIWS-extract and silver nitrate on (**a**) growth ((**1**) Silver nitrate, (**2**) RIWS-AgNP 7 (2 µg/ml), (**3**) RIWS-AgNP 7 (20 µg/ml), (**4**) RIWS-extract (200 µg/ml), (**5**) RIWS-AgNP 7 (200 µg/ml), (**6**) RIWS-AgNP 4 (2 µg/ml), (**7**) RIWS-AgNP 4 (20 µg/ml), (**8**) RIWS-AgNP 4 (200 µg/ml), (**9**) RIWS-AgNP 1 (2 µg/ml), (**10**) RIWS-AgNP 1 (20 µg/ml), (**11**) Control, (**12**) RIWS-AgNP 1 (200 µg/ml)), (**b, c**) seed germination index**,** root length, shoot length and root number and content of (**d**) Chlorophyll a, Chlorophyll b and total carotenoids in *Hordeum vulgare*. Values are mean ± standard deviation of three replicates

signaling pathways including cell proliferation, reactive oxygen species (ROS) scavenging and hormone signaling pathways [77, 79, 80]. Previous studies have also established that AgNPs regulates the expression of genes associated with secondary metabolism, cell cycle, carotenoid biosynthesis, antioxidant enzymes and metabolic pathway of phenolic compounds [77, 80–83]. In this study, the enhanced growth in *H. vulgare* might also be a consequence of increased concentration of photosynthetic pigments in seedlings after treatment with RIWS-AgNPs (Fig. 7d). The present findings revealed that 200 µg/ml of RIWS extract-derived AgNPs (RIWS-AgNP 1) could be effectively used as a green nano-biotechnological source to increase the yield and productivity of *H. vulgare*. The present study also suggests that nano-biotechnological interventions hold promising future prospects in agriculture sector.

Antioxidant activity of RIWS-AgNPs

DPPH assay is widely used for determining the antioxidant activity of natural compounds [84]. The present study compared the antioxidant activity of RIWS-AgNPs, RIWS-extract and standards (BHT and Rutin). The RIWS-AgNPs showed significantly higher antioxidant activity, as compared to RIWS-extract and BHT at 2–100 µg/ml concentrations ($p \leq 0.05$, Fig. 8a). The IC_{50} value (µg/ml) of RIWS-extract, RIWS-AgNPs, BHT and Rutin was observed to be 12.47, 12.30, 12.43 and 12.36, respectively (Fig. 8b). The EC_{50} value (mg/ml) of RIWS-extract, RIWS-AgNPs, BHT and Rutin was calculated to be 0.106, 0.104, 0.105 and 0.105, respectively (Fig. 8c). The ARP value of RIWS-extract, RIWS-AgNPs, BHT and Rutin was found to be 947.02, 959.45, 952.38 and 952.39, respectively (Fig. 8d). The higher antioxidant activity of RIWS-AgNPs might be attributed to the fact that AgNPs are capped with the bioactive compounds of the RIWS-extract that does not readily lose electrons, as compared to the bioactive compounds in the plant extract alone [34–37, 39–42, 85]. Similarly, several researchers have reported that the antioxidant activity of the plant extract-derived AgNPs is significantly higher as compared to the plant extract alone [86]. In this present study, the antioxidant activity of RIWS-extract and RIWS-AgNPs was found to increase in a concentration-dependent manner. The results suggest that the RIWS-AgNPs might be used as a potent antioxidant agent in different pharmacological formulations for ameliorating free radical-associated disorders, including cancer, atherosclerosis, diabetes and neurodegenerative diseases [87].

Cytotoxic activity of RIWS-AgNPs

Hepatocellular carcinoma is the third leading cause of cancer-related deaths globally [88]. World Health Organization estimates that every year 7,88,000 people die from primary liver cancer [89]. According to International Agency for Research on Cancer, the global burden of new cancer cases are expected to reach 27.5 million by 2040 [90]. Moreover, the global industry of cancer treatment is estimated to increase by $ 150 billion in 2020 [91]. Radiotherapy, surgery and chemotherapy are some of the conventional methods used for the treatment of cancer patients. However, the conventional cancer treatments have several drawbacks, including high recurrence rate, non-specificity, limited bioavailability, toxicity and other severe side effects that limit their clinical effectiveness [19]. In this context, the MNPs offer a promising platform for cancer theranostics due to

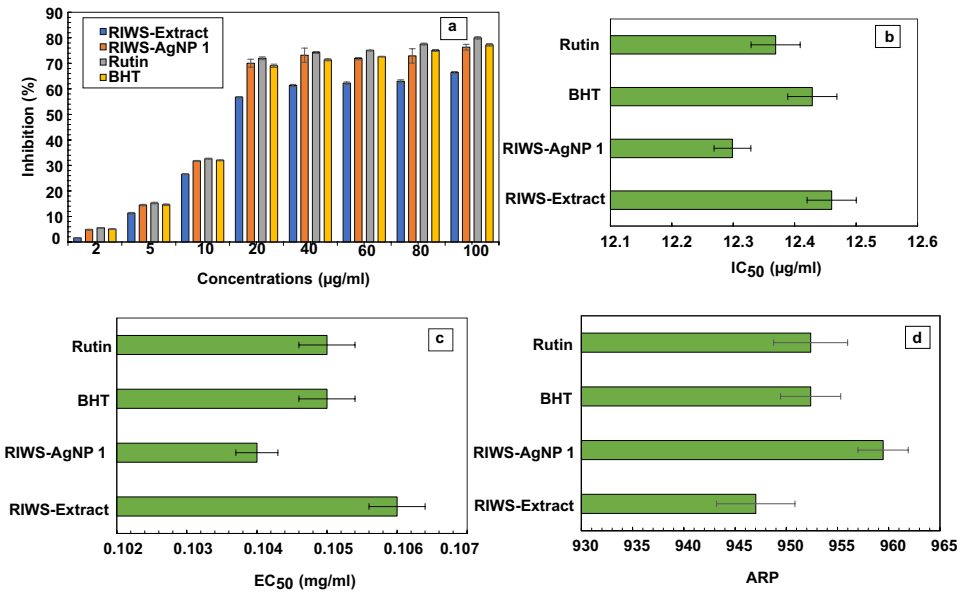

Fig. 8 DPPH free radical scavenging activity ((**a**) inhibition (%), (**b**) IC_{50}, (**c**) EC_{50} and (**d**) ARP) of RIWS-AgNP 1, RIWS-extract and standards (BHT and rutin). Values are mean ± standard deviation of three replicates

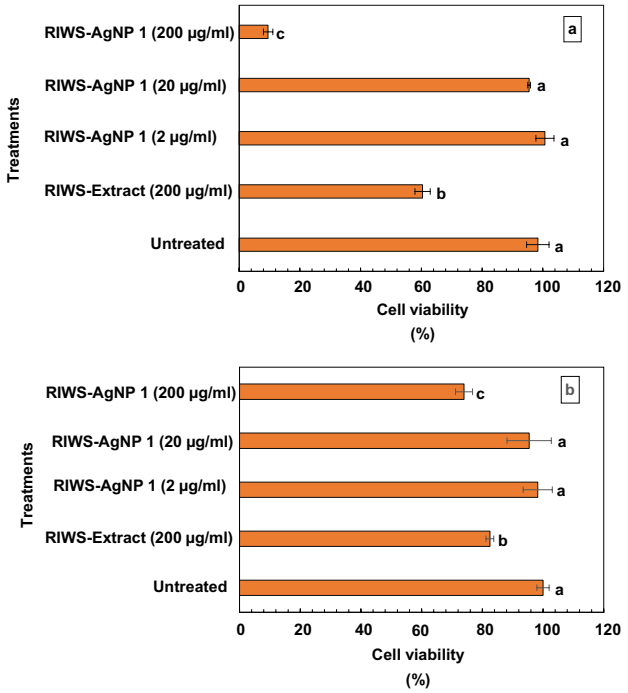

Fig. 9 In vitro cytotoxic activity of RIWS-extract derived AgNPs (RIWS-AgNP 1—RIWS-AgNP 3) and RIWS-extract against (**a**) HepG2 cancer cell line and (**b**) normal Huh7 cell line. Values are mean ± standard deviation of three replicates. Means with different letters are significantly different at $p \leq 0.05$ according to Bonferroni post hoc test

their unique physicochemical properties, high surface area to volume ratio, high permeability, low cost and high stability in biological fluids [92]. As shown in Fig. 9a, the RIWS-AgNPs showed high cytotoxicity against HepG2 cell line (RIWS AgNPs 1 (200 µg/ml) Cell viability: 9.51 ± 1.55%), as compared to RIWS-extract (Cell viability: 60.39 ± 2.51%; $p \leq 0.05$). Moreover, there is a gradual increase in cytotoxicity with concomitant increase in concentration of RIWS-AgNPs (Fig. 9a). Furthermore, RIWS-AgNPs showed limited cytotoxicity (RIWS AgNPs 1 (200 µg/ml) Cell viability: 78.25 ± 1.25%) against normal Huh7 cell line (Fig. 9b). This increased cytotoxicity activity of RIWS-AgNPs against HepG2 cancer cell line might be attributed to the generation of ROS, disruption of mitochondrial respiratory chain, G2/M or sub-G1 cell cycle arrest and decreased cellular ATP content [92]. Several authors have also suggested a down-regulation of DNA-dependent protein kinase and Bcl-2 gene and upregulation of Bax gene and p53 by biogenic AgNPs [93]. This strong cytotoxicity of RIWS-AgNPs could also be attributed to high antioxidant activity of these MNPs as reported in this study (Fig. 8). Several researchers have reported a significant correlation between the antioxidant activity and anticancer efficacy [94]. The results suggest that the cytotoxicity of RIWS-AgNPs increased in a concentration-dependent manner. Sahu et al. [95] also reported a concentration-dependent cytotoxicity of AgNPs against HepG2 cell line. The present findings suggest that the RIWS-AgNPs are biocompatible and could potentially be used as a chemotherapeutic agent in the near future.

Conclusion

In this present investigation, we have successfully established a safe, simple, economical and environment-friendly green approach for biosynthesis of RIWS-extract capped silver nanoparticles (RIWS-AgNPs) with pronounced bioactivities (antioxidant and anticancer) and diverse industrial applications. The various analytical techniques (UV–Vis, FTIR, TEM, DLS and SAED) have unveiled that equal ratio of $AgNO_3$ (1 mM) and RIWS-extract (1 mg/ml) is most favorable for the synthesis of small size, well dispersed, crystalline and stable RIWS-AgNPs. The findings of this present study suggest that phytosynthesized RIWS-AgNPs have tremendous potential in mitigating environmental pollution by promoting effective degradation of hazardous organic pollutant (4-nitrophenol). The present findings demonstrated that RIWS-AgNPs exert concentration-dependent antioxidant activity and cytotoxicity against HepG2 cancer cell line. Moreover, RIWS-AgNPs also enhanced the seed germination, growth and photosynthetic pigments of *Hordeum vulgare* in concentration and size-dependent manner. The results suggest that phytosynthesized RIWS-AgNPs have promising prospects in cancer therapeutics, ameliorating free-radical-associated health maladies, and boosting agro-economy. The future studies need to be focused on understanding the mechanism of action of RIWS-AgNPs.

Acknowledgements The authors wish to acknowledge Defence Research & Development Organization (DRDO), Ministry of Defence, Government of India, for financial support. Authors also wish to acknowledge Aastha Khullar (Department of Rheumatology, PGIMER, Chandigarh), Pankhuri Narula (Kusuma school of biological sciences, IIT, Delhi), Pulkit Bindra (INST, Chandigarh), Rajendra Kumar Singh (DIHAR, DRDO), Gurudev Singh (Department of Botany, Panjab University, Chandigarh), Dr. Archana Bhatnagar (Department of Biochemistry, Panjab University, Chandigarh) and SAIF Department (Panjab University (Chandigarh), AIIMS (Delhi) and IIT Delhi). The authors are also grateful to Rashmi Gupta and Ankit khullar for copy-editing of the manuscript.

Author contributions Conceptualization: SK; methodology: SK; formal analysis and investigation: SK; writing—original draft preparation: SK; writing—review and editing: SK and HS; funding acquisition: OPC; resources: SK, HS, SS and OPC and supervision: HS, SS and OPC.

Funding This study was funded by Defence Research & Development Organization (DRDO), Ministry of Defence, Government of India.

Declarations

Conflict of interest The authors declare that they have no conflict of interest.

Ethical approval This article does not contain any studies with human participants or animals performed by any of the authors.

Informed consent This article does not contain any studies with human participants performed by any of the authors.

References

1. Ahmed S, Ahmad M, Swami BL, Ikram S (2016) A review on plants extract mediated synthesis of silver nanoparticles for antimicrobial applications: a green expertise. J Adv Res 7:17–28. https://doi.org/10.1016/j.jare.2015.02.007
2. Larue C, Castillo-Michel H, Sobanska S et al (2014) Foliar exposure of the crop *Lactuca sativa* to silver nanoparticles: evidence for internalization and changes in Ag speciation. J Hazard Mater 264:98–106. https://doi.org/10.1016/j.jhazmat.2013.10.053
3. Mohasseli V, Farbood F, Moradi A (2020) Antioxidant defense and metabolic responses of lemon balm (*Melissa officinalis* L.) to Fe-nano-particles under reduced irrigation regimes. Ind Crops Prod 149:112338. https://doi.org/10.1016/j.indcrop.2020.112338
4. Islam NU, Jalil K, Shahid M et al (2019) Green synthesis and biological activities of gold nanoparticles functionalized with *Salix alba*. Arab J Chem 12:2914–2925. https://doi.org/10.1016/j.arabjc.2015.06.025
5. Yokoyama K, Welchons DR (2007) The conjugation of amyloid beta protein on the gold colloidal nanoparticles' surfaces. Nanotechnology 18:105101. https://doi.org/10.1088/0957-4484/18/10/105101
6. Wang J, Wang Z (2007) Rapid synthesis of hexagon-shaped gold nanoplates by microwave assistant method. Mater Lett 61:4149–4151. https://doi.org/10.1016/j.matlet.2007.01.043
7. Sharma VK, Yngard RA, Lin Y (2009) Silver nanoparticles: green synthesis and their antimicrobial activities. Adv Colloid Interface Sci 145:83–96. https://doi.org/10.1016/j.cis.2008.09.002
8. Hembram KC, Kumar R, Kandha L et al (2018) Therapeutic prospective of plant-induced silver nanoparticles: application as antimicrobial and anticancer agent. Artif Cells Nanomed Biotechnol 46:S38–S51. https://doi.org/10.1080/21691401.2018.1489262
9. Alharbi NS, Govindarajan M, Kadaikunnan S et al (2018) Nanosilver crystals capped with *Bauhinia acuminata* phytochemicals as new antimicrobials and mosquito larvicides. J Trace Elem Med Biol 50:146–153. https://doi.org/10.1016/j.jtemb.2018.06.016
10. El-Temsah YS, Joner EJ (2012) Impact of Fe and Ag nanoparticles on seed germination and differences in bioavailability during exposure in aqueous suspension and soil. Environ Toxicol 27:42–49. https://doi.org/10.1002/tox.20610
11. Kumari M, Mukherjee A, Chandrasekaran N (2009) Genotoxicity of silver nanoparticles in *Allium cepa*. Sci Total Environ 407:5243–5246. https://doi.org/10.1016/j.scitotenv.2009.06.024
12. Eby DM, Luckarift HR, Johnson GR (2009) Hybrid antimicrobial enzyme and silver nanoparticle coatings for medical instruments. ACS Appl Mater Interfaces 1:1553–1560. https://doi.org/10.1021/am9002155
13. Mukherjee P, Roy M, Mandal BP et al (2008) Green synthesis of highly stabilized nanocrystalline silver particles by a non-pathogenic and agriculturally important fungus *T. asperellum*. Nanotechnology 19:75103. https://doi.org/10.1088/0957-4484/19/7/075103
14. Zou T, Percival SS, Cheng Q et al (2012) Preparation, characterization, and induction of cell apoptosis of cocoa procyanidins–gelatin–chitosan nanoparticles. Eur J Pharm Biopharm 82:36–42. https://doi.org/10.1016/j.ejpb.2012.05.006
15. Sepeur S (2008) Nanotechnology: technical basics and applications. Vincentz Network, Germany
16. Mukherjee S, Chowdhury D, Kotcherlakota R et al (2014) Potential theranostics application of bio-synthesized silver nanoparticles (4-in-1 system). Theranostics 4:316–335. https://doi.org/10.7150/thno.7819
17. Abbasi E, Milani M, Aval SF et al (2016) Silver nanoparticles: Synthesis methods, bio-applications and properties. Crit Rev Microbiol 42:173–180. https://doi.org/10.3109/1040841X.2014.912200
18. Ahmad A, Wei Y, Syed F et al (2016) *Isatis tinctoria* mediated synthesis of amphotericin B-bound silver nanoparticles with enhanced photoinduced antileishmanial activity: a novel green approach. J Photochem Photobiol B Biol 161:17–24. https://doi.org/10.1016/j.jphotobiol.2016.05.003
19. Ovais M, Khalil AT, Raza A et al (2016) Green synthesis of silver nanoparticles via plant extracts: beginning a new era in cancer theranostics. Nanomedicine 11:3157–3177. https://doi.org/10.2217/nnm-2016-0279
20. Mittal J, Batra A, Singh A, Sharma MM (2014) Phytofabrication of nanoparticles through plant as nanofactories. Adv Nat Sci Nanosci Nanotechnol 5:43002. https://doi.org/10.1088/2043-6262/5/4/043002
21. Rajeshkumar S, Bharath LV (2017) Mechanism of plant-mediated synthesis of silver nanoparticles—a review on biomolecules involved, characterisation and antibacterial activity. Chem Biol Interact 273:219–227. https://doi.org/10.1016/j.cbi.2017.06.019
22. Jadhav K, Dhamecha D, Bhattacharya D, Patil M (2016) Green and ecofriendly synthesis of silver nanoparticles: characterization, biocompatibility studies and gel formulation for treatment of infections in burns. J Photochem Photobiol B Biol 155:109–115. https://doi.org/10.1016/j.jphotobiol.2016.01.002
23. Ajitha B, Reddy YAK, Reddy PS (2015) Biosynthesis of silver nanoparticles using *Momordica charantia* leaf broth: evaluation of their innate antimicrobial and catalytic activities. J Photochem Photobiol B Biol 146:1–9. https://doi.org/10.1016/j.jphotobiol.2015.02.017
24. Patra JK, Das G, Baek K-H (2016) Phyto-mediated biosynthesis of silver nanoparticles using the rind extract of watermelon (*Citrullus lanatus*) under photo-catalyzed condition and investigation of its antibacterial, anticandidal and antioxidant efficacy. J Photochem Photobiol B Biol 161:200–210. https://doi.org/10.1016/j.jphotobiol.2016.05.021
25. Baldi A, Singh D, Dixit VK (2008) Dual elicitation for improved production of Withaferin A by cell suspension cultures of *Withania somnifera*. Appl Biochem Biotechnol 151:556. https://doi.org/10.1007/s12010-008-8231-2
26. Kumar A, Kaul MK, Bhan MK et al (2007) Morphological and chemical variation in 25 collections of the Indian medicinal plant, *Withania somnifera* (L.) Dunal (Solanaceae). Genet Resour Crop Evol 54:655–660. https://doi.org/10.1007/s10722-006-9129-x
27. Singh S, Sushil K (1998) *Withania somnifera*: the Indian Ginseng Ashwagandha. Central Institute of Medicinal and Aromatic Plants, Lucknow
28. Kumar A, Mir BA, Sehgal D et al (2011) Utility of a multidisciplinary approach for genome diagnostics of cultivated and wild germplasm resources of medicinal *Withania somnifera*, and the status of new species, W. *ashwagandha*, in the cultivated taxon. Plant Syst Evol 291:141–151. https://doi.org/10.1007/s00606-010-0372-4
29. Asthana R, Raina MK (1989) Pharmacology of *Withania somnifera* (L.) Dunal—a review. Indian Drugs 26:199–205

30. Fatima N, Ahmad N, Ahmad I, Anis M (2015) Interactive effects of growth regulators, carbon sources, pH on plant regeneration and assessment of genetic fidelity using single primer amplification reaction (SPARS) techniques in *Withania somnifera* L. Appl Biochem Biotechnol 177:118–136. https://doi.org/10.1007/s12010-015-1732-x
31. Sivanandhan G, Mariashibu TS, Arun M et al (2011) The effect of polyamines on the efficiency of multiplication and rooting of *Withania somnifera* (L.) Dunal and content of some withanolides in obtained plants. Acta Physiol Plant 33:2279. https://doi.org/10.1007/s11738-011-0768-y
32. Udayakumar R, Kasthurirengan S, Mariashibu TS et al (2014) Agrobacterium-mediated genetic transformation of *Withania somnifera* using nodal explants. Acta Physiol Plant 36:1969–1980. https://doi.org/10.1007/s11738-014-1572-2
33. Bhattacharya SK, Goel RK, Kaur R, Ghosal S (1987) Anti-stress activity of sitoindosides VII and VIII, new acylsterylglucosides from *Withania somnifera*. Phyther Res 1:32–37. https://doi.org/10.1002/ptr.2650010108
34. Das CN, Gupta VK, Sangwan RS (2007) Leaf ontogenic phase-related dynamics of withaferin a and withanone biogenesis in ashwagandha (*Withania somnifera* Dunal.)—an important medicinal herb. J Plant Biol 50:508. https://doi.org/10.1007/BF03030691
35. Nur-e-Alam M, Yousaf M, Qureshi S et al (2003) A novel Dimeric Podophyllotoxin-type lignan and a new Withanolide from *Withania coagulans*. Helv Chim Acta 86:607–614. https://doi.org/10.1002/hlca.200390060
36. Chatterjee S, Srivastava S, Khalid A et al (2010) Comprehensive metabolic fingerprinting of *Withania somnifera* leaf and root extracts. Phytochemistry 71:1085–1094. https://doi.org/10.1016/j.phytochem.2010.04.001
37. Choudhary A, Kumar R, Srivastava RB et al (2015) Isolation and characterization of phenolic compounds from *Rhodiola imbricata*, a Trans-Himalayan food crop having antioxidant and anticancer potential. J Funct Foods 16:183–193. https://doi.org/10.1016/j.jff.2015.04.013
38. Kapoor S, Raghuvanshi R, Bhardwaj P et al (2018) Influence of light quality on growth, secondary metabolites production and antioxidant activity in callus culture of *Rhodiola imbricata* Edgew. J Photochem Photobiol B Biol 183:258–265. https://doi.org/10.1016/j.jphotobiol.2018.04.018
39. Chawla R, Jaiswal S, Kumar R et al (2010) Himalayan Bioresource *Rhodiola imbricata* as a promising radioprotector for nuclear and radiological emergencies. J Pharm Bioallied Sci 2:213–219. https://doi.org/10.4103/0975-7406.68503
40. Gupta V, Lahiri SS, Sultana S et al (2010) Anti-oxidative effect of *Rhodiola imbricata* root extract in rats during cold, hypoxia and restraint (C-H-R) exposure and post-stress recovery. Food Chem Toxicol 48:1019–1025. https://doi.org/10.1016/j.fct.2010.01.012
41. Senthilkumar R, Chandran R, Parimelazhagan T (2014) Hepatoprotective effect of *Rhodiola imbricata* rhizome against paracetamol-induced liver toxicity in rats. Saudi J Biol Sci 21:409–416. https://doi.org/10.1016/j.sjbs.2014.04.001
42. Tayade AB, Dhar P, Kumar J et al (2013) Chemometric profile of root extracts of *Rhodiola imbricata* Edgew. With hyphenated gas chromatography mass spectrometric technique. PLoS ONE. https://doi.org/10.1371/journal.pone.0052797
43. Gupta V, Saggu S, Tulsawani RK et al (2008) A dose dependent adaptogenic and safety evaluation of *Rhodiola imbricata* Edgew, a high altitude rhizome. Food Chem Toxicol 46:1645–1652. https://doi.org/10.1016/j.fct.2007.12.027
44. Khanna K, Mishra KP, Ganju L, Singh SB (2017) Golden root: a wholesome treat of immunity. Biomed Pharmacother 87:496–502. https://doi.org/10.1016/j.biopha.2016.12.132
45. Tayade AB, Dhar P, Kumar J et al (2017) Trans-Himalayan *Rhodiola imbricata* Edgew. root: a novel source of dietary amino acids, fatty acids and minerals. J Food Sci Technol 54:359–367. https://doi.org/10.1007/s13197-016-2469-4
46. Tayade AB, Dhar P, Kumar J et al (2013) Sequential determination of fat- and water-soluble vitamins in *Rhodiola imbricata* root from trans-Himalaya with rapid resolution liquid chromatography/tandem mass spectrometry. Anal Chim Acta 789:65–73. https://doi.org/10.1016/j.aca.2013.05.062
47. Nakkala JR, Mata R, Raja K et al (2018) Green synthesized silver nanoparticles: catalytic dye degradation, in vitro anticancer activity and in vivo toxicity in rats. Mater Sci Eng C 91:372–381. https://doi.org/10.1016/j.msec.2018.05.048
48. Lichtenthaler HK, Buschmann C (2001) Chlorophylls and carotenoids: measurement and characterization by UV–VIS spectroscopy. Curr Protoc Food Anal Chem 1:F4.3.1-F4.3.8. https://doi.org/10.1002/0471142913.faf0403s01
49. Choi CW, Kim SC, Hwang SS et al (2002) Antioxidant activity and free radical scavenging capacity between Korean medicinal plants and flavonoids by assay-guided comparison. Plant Sci 163:1161–1168. https://doi.org/10.1016/S0168-9452(02)00332-1
50. Prakash D, Upadhyay G, Singh BN, Singh HB (2007) Antioxidant and free radical-scavenging activities of seeds and agri-wastes of some varieties of soybean (*Glycine max*). Food Chem 104:783–790. https://doi.org/10.1016/j.foodchem.2006.12.029
51. Kroyer GT (2004) Red clover extract as antioxidant active and functional food ingredient. Innov Food Sci Emerg Technol 5:101–105. https://doi.org/10.1016/S1466-8564(03)00040-7
52. Dajanta K, Apichartsrangkoon A, Chukeatirote E (2011) Antioxidant properties and total phenolics of Thua Nao (a Thai Fermented Soybean)as affected by Bacillus-fermentation. J Microb Biochem Technol 03:56–59. https://doi.org/10.4172/1948-5948.1000052
53. Mosmann T (1983) Rapid colorimetric assay for cellular growth and survival: application to proliferation and cytotoxicity assays. J Immunol Methods 65:55–63. https://doi.org/10.1016/0022-1759(83)90303-4
54. Forthofer RN, Lee ES, Hernandez M (2007) 6—Study designs. In: Forthofer RN, Lee ES, Hernandez MBT-B, Second E (eds) Biostatistics: a guide to design, analysis and discovery. Academic Press, San Diego: 135–167. https://www.sciencedirect.com/book/9780123694928/biostatistics?via=ihub=#book-description
55. Padmos JD, Boudreau RTM, Weaver DF, Zhang P (2015) Impact of protecting ligands on surface structure and antibacterial activity of silver nanoparticles. Langmuir 31:3745–3752. https://doi.org/10.1021/acs.langmuir.5b00049
56. Mulvaney P (1996) Surface plasmon spectroscopy of nanosized metal particles. Langmuir 12:788–800. https://doi.org/10.1021/la9502711
57. Prathna TC, Chandrasekaran N, Raichur AM, Mukherjee A (2011) Biomimetic synthesis of silver nanoparticles by *Citrus limon* (lemon) aqueous extract and theoretical prediction of particle size. Colloids Surfaces B Biointerfaces 82:152–159. https://doi.org/10.1016/j.colsurfb.2010.08.036
58. Mittal AK, Chisti Y, Banerjee UC (2013) Synthesis of metallic nanoparticles using plant extracts. Biotechnol Adv 31:346–356. https://doi.org/10.1016/j.biotechadv.2013.01.003
59. Stetefeld J, McKenna SA, Patel TR (2016) Dynamic light scattering: a practical guide and applications in biomedical sciences. Biophys Rev 8:409–427. https://doi.org/10.1007/s12551-016-0218-6
60. Bastos Araruna F, Oliveira Sousa Araruna F, Lima Alves Pereira LP et al (2020) Green syntheses of silver nanoparticles using babassu mesocarp starch (Attalea speciosa Mart. ex Spreng.) and their antimicrobial applications. Environ Nanotechnol Monit Manag 13:100281. https://doi.org/10.1016/j.enmm.2019.100281
61. Vijayaraghavan K, Nalini SPK, Prakash NU, Madhankumar D (2012) Biomimetic synthesis of silver nanoparticles by aqueous extract of *Syzygium aromaticum*. Mater Lett 75:33–35. https://doi.org/10.1016/j.matlet.2012.01.083

62. Jagtap UB, Bapat VA (2013) Green synthesis of silver nanoparticles using *Artocarpus heterophyllus* Lam. seed extract and its antibacterial activity. Ind Crops Prod 46:132–137. https://doi.org/10.1016/j.indcrop.2013.01.019
63. Awwad AM, Salem NM, Abdeen AO (2013) Green synthesis of silver nanoparticles using carob leaf extract and its antibacterial activity. Int J Ind Chem 4:29. https://doi.org/10.1186/2228-5547-4-29
64. Raut RW, Mendhulkar VD, Kashid SB (2014) Photosensitized synthesis of silver nanoparticles using *Withania somnifera* leaf powder and silver nitrate. J Photochem Photobiol B Biol 132:45–55. https://doi.org/10.1016/j.jphotobiol.2014.02.001
65. Panneerselvam C, Murugan K, Roni M et al (2016) Fern-synthesized nanoparticles in the fight against malaria: LC/MS analysis of *Pteridium aquilinum* leaf extract and biosynthesis of silver nanoparticles with high mosquitocidal and antiplasmodial activity. Parasitol Res 115:997–1013. https://doi.org/10.1007/s00436-015-4828-x
66. Paulkumar K, Gnanajobitha G, Vanaja M et al (2014) *Piper nigrum* leaf and stem assisted green synthesis of silver nanoparticles and evaluation of its antibacterial activity against agricultural plant pathogens. Sci World J 2014:829894. https://doi.org/10.1155/2014/829894
67. Chern J-M, Chien Y-W (2002) Adsorption of nitrophenol onto activated carbon: isotherms and breakthrough curves. Water Res 36:647–655. https://doi.org/10.1016/S0043-1354(01)00258-5
68. U.S. Environmental Protection Agency (2016) https://www.epa.gov/sites/production/files/2016-09/documents/4-nitrophenol.pdf. Accessed 06 Apr 2020
69. U.S. Environmental Protection Agency (2019) https://www.epa.gov/sites/production/files/2019-03/documents/ambient-wqc-nitrophenols-1980.pdf. Accessed 06 Apr 2020
70. Singh J, Kaur N, Kaur P et al (2018) Piper betle leaves mediated synthesis of biogenic SnO_2 nanoparticles for photocatalytic degradation of reactive yellow 186 dye under direct sunlight. Environ Nanotechnol Monit Manag 10:331–338. https://doi.org/10.1016/j.enmm.2018.07.001
71. Wu F, Yang Q (2011) Ammonium bicarbonate reduction route to uniform gold nanoparticles and their applications in catalysis and surface-enhanced Raman scattering. Nano Res 4:861–869. https://doi.org/10.1007/s12274-011-0142-9
72. Daniel M-C, Astruc D (2004) Gold nanoparticles: assembly, supramolecular chemistry, quantum-size-related properties, and applications toward biology, catalysis, and nanotechnology. Chem Rev 104:293–346. https://doi.org/10.1021/cr030698
73. Vella F (1995) Principles of bioinorganic chemistry pp 411. University Science Books, Mill Valley, California. 1994. Biochem Educ 23:115. https://doi.org/10.1016/0307-4412(95)90685-1
74. Sallam SA, Orabi AS, Abbas AM (2011) DNA interaction with octahedral and square planar Ni(II) complexes of aspartic-acid Schiff-bases. J Mol Struct 1006:272–281. https://doi.org/10.1016/j.molstruc.2011.09.020
75. Edison TJI, Sethuraman MG (2013) Biogenic robust synthesis of silver nanoparticles using *Punica granatum* peel and its application as a green catalyst for the reduction of an anthropogenic pollutant 4-nitrophenol. Spectrochim Acta Part A Mol Biomol Spectrosc 104:262–264. https://doi.org/10.1016/j.saa.2012.11.084
76. Francis S, Joseph S, Koshy EP, Mathew B (2018) Microwave assisted green synthesis of silver nanoparticles using leaf extract of *Elephantopus scaber* and its environmental and biological applications. Artif Cells Nanomed Biotechnol 46:795–804. https://doi.org/10.1080/21691401.2017.1345921
77. Gupta SD, Agarwal A, Pradhan S (2018) Phytostimulatory effect of silver nanoparticles (AgNPs) on rice seedling growth: an insight from antioxidative enzyme activities and gene expression patterns. Ecotoxicol Environ Saf 161:624–633. https://doi.org/10.1016/j.ecoenv.2018.06.023
78. Qian H, Peng X, Han X et al (2013) Comparison of the toxicity of silver nanoparticles and silver ions on the growth of terrestrial plant model *Arabidopsis thaliana*. J Environ Sci 25:1947–1956. https://doi.org/10.1016/S1001-0742(12)60301-5
79. Mirzajani F, Askari H, Hamzelou S et al (2013) Effect of silver nanoparticles on *Oryza sativa* L. and its rhizosphere bacteria. Ecotoxicol Environ Saf 88:48–54. https://doi.org/10.1016/j.ecoenv.2012.10.018
80. Syu Y, Hung J-H, Chen J-C, Chuang H (2014) Impacts of size and shape of silver nanoparticles on Arabidopsis plant growth and gene expression. Plant Physiol Biochem 83:57–64. https://doi.org/10.1016/j.plaphy.2014.07.010
81. Vannini C, Domingo G, Onelli E et al (2013) Morphological and proteomic responses of *Eruca sativa* exposed to silver nanoparticles or silver nitrate. PLoS ONE 8:7e68752
82. Thiruvengadam M, Gurunathan S, Chung I-M (2015) Physiological, metabolic, and transcriptional effects of biologically-synthesized silver nanoparticles in turnip (Brassica rapa ssp. rapa L.). Protoplasma 252:1031–1046. https://doi.org/10.1007/s00709-014-0738-5
83. Baskar V, Venkatesh J, Park SW (2015) Impact of biologically synthesized silver nanoparticles on the growth and physiological responses in *Brassica rapa* ssp. *pekinensis*. Environ Sci Pollut Res 22:17672–17682. https://doi.org/10.1007/s11356-015-4864-1
84. Shimada K, Fujikawa K, Yahara K, Nakamura T (1992) Antioxidative properties of xanthan on the autoxidation of soybean oil in cyclodextrin emulsion. J Agric Food Chem 40:945–948. https://doi.org/10.1021/jf00018a005
85. Kumar B, Smita K, Seqqat R et al (2016) In vitro evaluation of silver nanoparticles cytotoxicity on Hepatic cancer (Hep-G2) cell line and their antioxidant activity: Green approach for fabrication and application. J Photochem Photobiol B Biol 159:8–13. https://doi.org/10.1016/j.jphotobiol.2016.03.011
86. Abdel-Aziz MS, Shaheen MS, El-Nekeety AA, Abdel-Wahhab MA (2014) Antioxidant and antibacterial activity of silver nanoparticles biosynthesized using *Chenopodium murale* leaf extract. J Saudi Chem Soc 18:356–363. https://doi.org/10.1016/j.jscs.2013.09.011
87. Halliwell B, Gutteridge JMC (1984) Oxygen toxicity, oxygen radicals, transition metals and disease. Biochem J 219:1–14. https://doi.org/10.1042/bj2190001
88. Nakagawa H, Fujita M, Fujimoto A (2019) Genome sequencing analysis of liver cancer for precision medicine. Semin Cancer Biol 55:120–127. https://doi.org/10.1016/j.semcancer.2018.03.004
89. World Health Organization (2018) https://www.who.int/hepatitis/news-events/world-cancer-day/en/. Accessed 06 Apr 2020
90. American cancer society, Global cancer, Facts and figures 4th edition, USA (2018) https://www.cancer.org/content/dam/cancer-org/research/cancer-facts-and-statistics/global-cancer-facts-and-figures/global-cancer-facts-and-figures-4th-edition.pdf. Accessed 06 Apr 2020
91. I.I.f.H. Informatics (2016) http://www.imshealth.com/en/thought-leadership/ims-institute2016. Accessed 25 Feb 2018
92. Barabadi H, Alizadeh A, Ovais M et al (2018) Efficacy of green nanoparticles against cancerous and normal cell lines: a systematic review and meta-analysis. IET Nanobiotechnol 12:377–391. https://doi.org/10.1049/iet-nbt.2017.0120

93. Chahardoli A, Karimi N, Fattahi A (2018) Nigella arvensis leaf extract mediated green synthesis of silver nanoparticles: their characteristic properties and biological efficacy. Adv Powder Technol 29:202–210. https://doi.org/10.1016/j.apt.2017.11.003
94. Raghunandan D, Ravishankar B, Sharanbasava G et al (2011) Anti-cancer studies of noble metal nanoparticles synthesized using different plant extracts. Cancer Nanotechnol 2:57–65. https://doi.org/10.1007/s12645-011-0014-8
95. Sahu SC, Zheng J, Graham L et al (2014) Comparative cytotoxicity of nanosilver in human liver HepG2 and colon Caco2 cells in culture. J Appl Toxicol 34:1155–1166. https://doi.org/10.1002/jat.2994